JACS
JOURNAL OF THE AMERICAN CHEMICAL SOCIETY
pubs.acs.org/JACS

Article

Methane Catalytic Amidation via a Plausible Copper-Nitrene Intermediate

Jonathan Martínez-Laguna, Anna Cholewinska, Elena Borrego, Maria Besora,* María Álvarez,* Ana Caballero,* and Pedro J. Pérez*

Cite This: J. Am. Chem. Soc. 2026, 148, 9057−9065

Read Online

ACCESS | Metrics & More | Article Recommendations | Supporting Information

ABSTRACT: The catalytic conversion of CH_4 into CH_3X compounds has been reported in a few cases, usually involving dehydrogenative processes in which the H atom is lost. Aiming at expanding this limited set of transformations, we have investigated the methane amidation reaction through metal-catalyzed nitrene transfer reactions, a transformation that remains unreported to date for the lightest hydrocarbon. Herein, we describe the use of copper-based catalysts for the direct, nondehydrogenative amidation reaction of methane via a metal-mediated formal nitrene insertion into the C−H bond, a reaction that is also extended to the series of gaseous alkanes. Mechanistic studies, supported by DFT calculations, a microkinetic model, and experimental evidence have led to the proposal of a metallonitrene intermediate responsible for this C−H amidation process via sequential hydrogen abstraction and rebound steps.

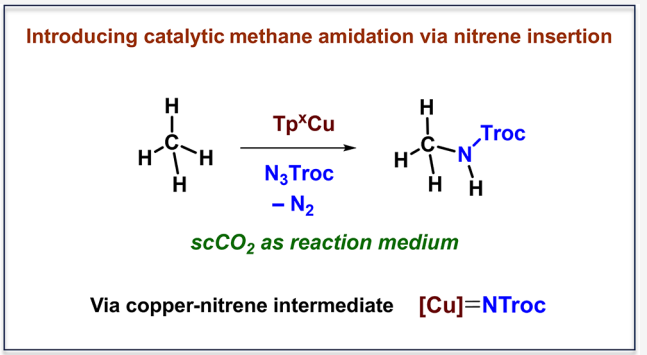

INTRODUCTION

The direct functionalization of methane remains a major challenge in modern chemistry[1,2] primarily due to the exceptional stability of its C−H bond, which possesses the highest bond dissociation energy among alkanes[3] and a poor polarity.[4] These factors lead to two major drawbacks: an inherent low reactivity and, once reacted, the appearance of selectivity issues, since very frequently the product contains C−H bonds more reactive than those of the parent methane. Despite these problems, there are a few examples in which the homogeneous metal-catalyzed functionalization of methane has been achieved upon generating C−O,[5,6] C−B,[7,8] C−Si,[9] or C−C[10] bonds. Of particular interest is the oxidation into methanol involving the intermediacy of metal-oxo species M═O (Scheme 1a),[11] which display a very high electrophilicity that facilitates the reaction with the methane C−H bond, a rather poor nucleophile. Interestingly, the analogous methane amidation reaction via nitrene transfer remains unreported, a transformation that should take place via similar metal-nitrene intermediates M═NR (Scheme 1a).[12]

To date, examples of metal-catalyzed methane amination/amidation have been reduced to a few (Scheme 1b). Crabtree first reported the formation of methyl radicals employing Hg/hν in the reaction of methane and ammonia, leading to methylamine.[13] More recently, Guo described the amidation of methane using cerium-based photocatalysts and hydrazines as nitrogen sources.[14] Later, in a thermal transformation, Hartwig and Pérez reported the copper-based methane amidation in the presence of peroxides.[15] It is noted that these three transformations correspond to dehydrogenative processes, implying the formal loss of hydrogen from the substrates as well as the formation of methyl radicals upon hydrogen abstraction, either photochemically or peroxide-induced. Stoichiometric metal-driven methane amination is also known.[16]

The metal-catalyzed transfer of nitrene to C−H bonds constitutes an alternative route for the above goal. However, whereas this strategy has been successfully applied for condensed alkanes,[17−19] it was not until the recent seminal work by Chang[20] that light alkanes C2−C4 were amidated, employing a cobalt-based catalyst and an azide (N_3Troc; Troc = $-C(O)OCH_2CCl_3$) as the nitrene source (Scheme 1c). Selectivity was preferred toward secondary sites using propane or butane. After this breakthrough, methane remains the only alkane that has not been amidated via nitrene-transfer reactions. Therefore, we have targeted this goal following our previous investigations on the use of coinage metal complexes bearing trispyrazolylborate ligands for the transfer of NTs (Ts = *p*-toluenesulfonate) units from PhI═NTs to saturated bonds.[17,21,22] With the appropriate combination of the Tp^x

Received: December 18, 2025
Revised: January 27, 2026
Accepted: February 2, 2026
Published: February 19, 2026

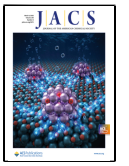

https://doi.org/10.1021/jacs.5c22747
J. Am. Chem. Soc. 2026, 148, 9057−9065

Scheme 1. Methane Catalytic Amidation[a]

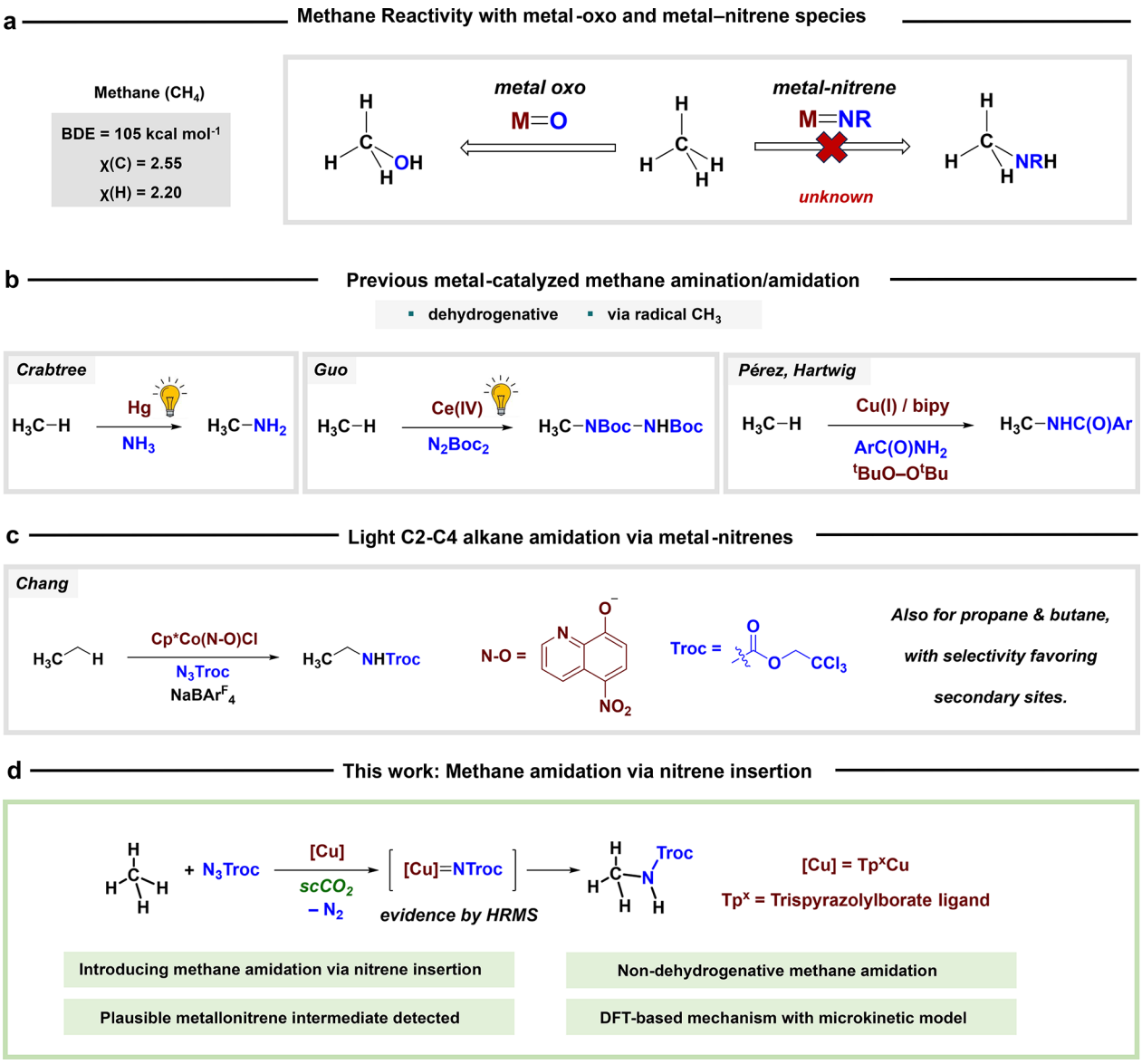

[a](a) Metal-oxo and metal-nitrene reactive species for methane functionalization. (b) Previous examples for dehydrogenative methane amidation via methyl radicals. (c) Chang's seminal work for gaseous C2−C4 alkanes C−H bond amidation by catalytic nitrene transfer. (d) This work: methane amidation via nitrene insertion.

ligand, the metal (copper), and the nitrene source (N_3Troc), we herein describe the first example of the direct amidation of methane via formal nitrene insertion into the C−H bond of the lightest alkane (Scheme 1d). The reaction proceeds via a copper-nitrene intermediate that has been detected by mass spectrometry, a species predicted by DFT calculations. Expansion to C2−C4 alkanes has been explored as well, with high success.

RESULTS AND DISCUSSION

Catalytic Amidation of Alkanes

We first evaluated the capabilities of several Cu- and Ag-based complexes to transfer the NTroc moiety to the C−H bond of cyclohexane as the probe reaction (Scheme 2a). Among the complexes tested, those containing copper and Tp^x ligands led to the best conversions into C_6H_{11}−N(H)Troc (**1**), the product derived from the insertion of the NTroc unit into the cyclohexane C−H bond (see SI for the optimization of reaction conditions). It is also noteworthy that the use of N_3Ts or other azides proved to be ineffective (see SI), assessing the singular behavior of N_3Troc. The mass balance is completed with NTroc-derived products due to decomposition pathways previously reported by Chang in his seminal contribution.[20] The main byproduct is 2,2,2-trichloroethyl carbamate (>80% of byproducts), with very minor amounts (<20% of byproducts) of 2,2,2-trichloroethanol, methyl carbamate, methyl alkyl carbamates, alkyl isocyanate, and alkyl chlorides (see SI). The order of reactivity for the Cu-based catalysts is $Tp^* < Tp^{*,Br} < Tp^{(CF3)2,Br} < Tp^{Ms} < Tp^{CF3} < Tp^{Br3}$. We have previously found[18] that for nitrene transfer reactions using Tp^xM cores (M = Cu, Ag), an increase in electrophilicity provides better results, albeit an excess of electron deficiency results in a decrease of chemoselectivity, since decomposition pathways are also enhanced.

https://doi.org/10.1021/jacs.5c22747
J. Am. Chem. Soc. 2026, 148, 9057−9065

Scheme 2. Alkane Amidation via Copper-Catalyzed Nitrene Transfer from Azide[a]

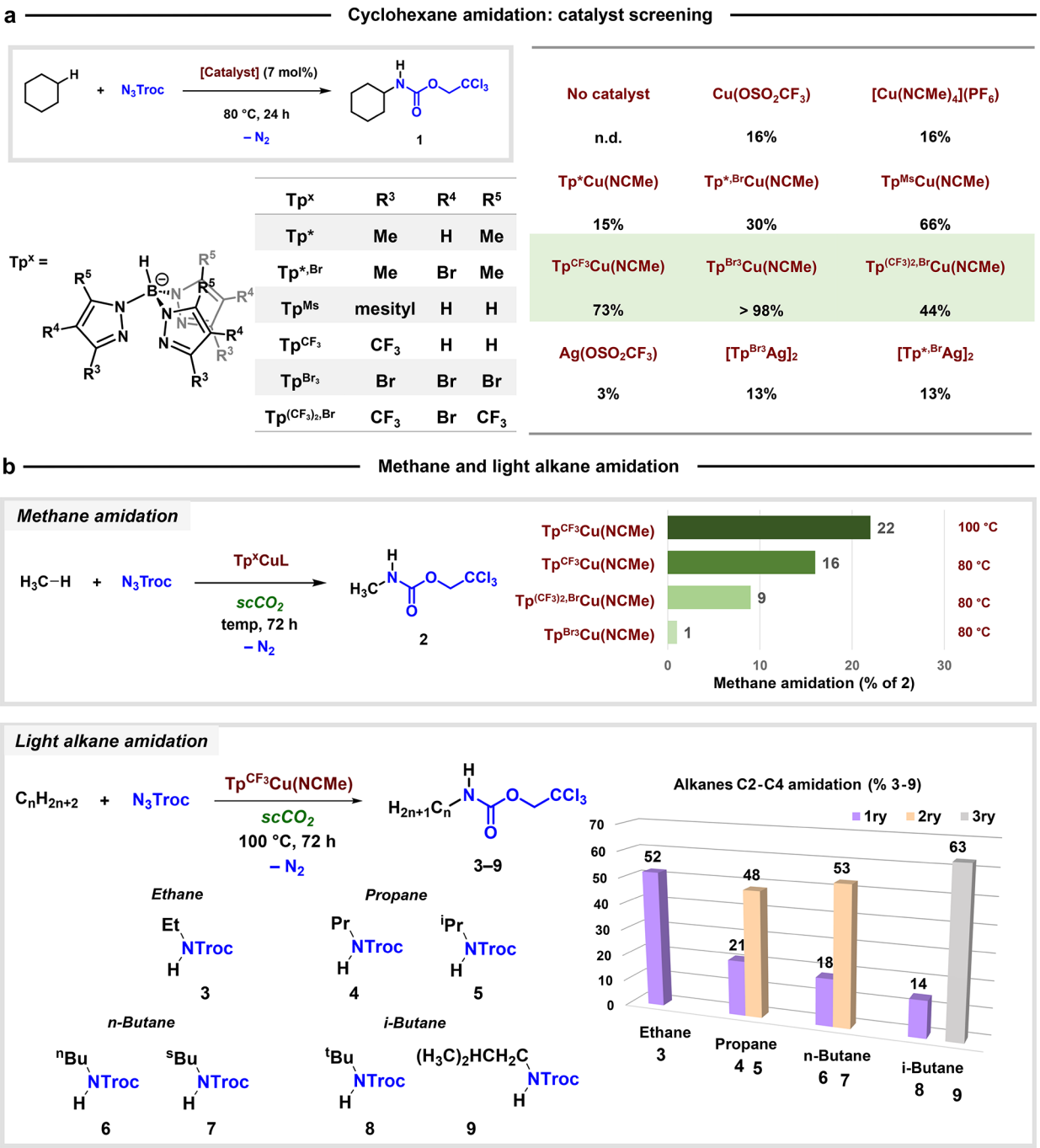

[a](a) Cyclohexane probe reaction for catalyst screening. (b) Methane and light alkane amidation. All yields are referred to as the initial azide.

This would explain why the $Tp^{(CF3)2,Br}$-based catalyst is less effective than $Tp^{Br3}Cu$.

Once the viability of the Tp^xCu-N_3Troc system was demonstrated with cyclohexane, we moved to light alkanes (Scheme 2b). Given the high bond dissociation energies of these hydrocarbons,[3] the selection of the solvent is crucial: the highly reactive metal-nitrene intermediates might react with any nucleophile present in the reaction medium rather than with the targeted alkane. To address this issue, we have employed supercritical carbon dioxide, ensuring a one-phase medium with no other possible reaction site than the alkane C−H bond.[23] The use of $scCO_2$ as a solvent is becoming routine, and many homogeneous catalytic systems have already been described in such a medium.[24] With methane as the reactant, we tested three Tp^xCu catalysts differing in their ancillary ligand. The best results were obtained with $Tp^{CF3}Cu(NCMe)$, which leads to a 22% yield (azide-based) of $CH_3-N(H)CO_2CH_2CCl_3$ (**2**) in the first example of methane amidation by nitrene insertion. The poor performance of the Tp^{Br3}-containing catalyst is explained due to its low solubility in the $scCO_2-CH_4$ medium, whereas both $Tp^{CF3}Cu$ and $Tp^{(CF3)2,Br}Cu$ complexes are soluble in such a mixture. The mass balance was completed with azide-derived decomposition products (see SI).

https://doi.org/10.1021/jacs.5c22747
J. Am. Chem. Soc. 2026, 148, 9057−9065

Alkanes C2−C4 were also evaluated in $scCO_2$, with yields (based on initial azide) ranging from 52% (ethane) to 77% (iso-butane). The selectivities favor the secondary (propane, butane) or tertiary (iso-butane) sites, albeit the functionalization of the primary sites takes place to a higher degree compared to the cobalt system reported by Chang.[20] Accordingly, the selectivities for primary (1ry) and secondary (2ry) sites for propane and butane with the copper catalyst are 1:7 and 1:4.4, respectively. These values are statistically corrected with the number of hydrogens of each type in the alkane. The cobalt catalyst provided 1:24 for propane and 1:16 for butane. We have also evaluated iso-butane, which generates a mixture of the two products derived from the functionalization of the primary and tertiary sites, with a corrected selectivity of 1:20. Overall, the reactivity observed follows the order C−H primary (1ry) < C−H secondary (2ry) < C−H tertiary (3ry).

Back to methane as the substrate, we first evaluated the effect of the pressure on the reaction outcome, carrying out additional experiments with 50 and 100 bar of CH_4 in $scCO_2$ as the solvent. Scheme 3a shows the variation of the yield of **2** with methane pressure, with a linear correlation being found. In another set of experiments, using 160 bar of methane, the reaction was monitored with time. Eight identical experiments were run and analyzed at 3, 6, 10, 16, 24, 48, 72, and 100 h, with the results shown in Scheme 3b. The yield increases up to ca. 60 h, and after 80 h, the reaction is finished. The average TOF, calculated at 80 h, is 5.5×10^{-4} mmol **2** h^{-1}. These data will be employed to develop the microkinetic model (see below).

The observation of a decrease in yields from cyclohexane to methane can be explained by two factors. On one hand, there is a difference in their C−H bond dissociation energies, with cyclohexane being 6 kcal mol^{-1} lower than methane.[3] On the other hand, the concentration of the alkane is much higher when using a liquid hydrocarbon than when using a $scCO_2$−CH_4 mixture. To compare the relative reactivity of methane and cyclohexane, an experiment in $scCO_2$ using 92 mmol of cyclohexane and 260 mmol of methane was carried out. The main product was the cyclohexyl derivative (Scheme 3c), with <1% yield of **2** being quantified (see SI for details).

DFT Calculations

We have performed DFT calculations (B3LYP-D3/def2TZVP&def2QZVP-SMD//B3LYP-D3/6−31g(d)&LANL2DZ-SMD, see full details in SI) to elucidate the reaction mechanism for the methane amidation process. All computational results are available in the ioChem-BD repository[25] and can be accessed via https://iochem-bd.urv.es/browse/handle/100/2265. Scheme 4 shows the reaction free energy profile. A microkinetic model has been built using the computational free energies and mechanism (see SI for details). The catalyst precursor $Tp^{CF3}Cu(NCMe)$ (**Int0**^{S}) first dissociates MeCN, leading to intermediate **Int1**^{S}, which is 11.6 kcal mol^{-1} less stable than **Int0**^{S}. The azide N_3Troc coordinates to **Int1**^{S}, a step that may form two species depending on the atom coordinated to copper: the internal nitrogen of azide (**Int2**$_N^S$) or the carbonyl oxygen (**Int2**$_O^S$). The lack of added acetonitrile and the relatively high concentration of N_3Troc help their formation even though their energies are relatively high, −1.9 for **Int2**$_N^S$ and 0.9 kcal mol^{-1} for **Int2**$_O^S$ with respect to **Int1**^{S}. The transient concentrations during the first 24 h range between 3.0×10^{-3} and 2.6×10^{-3} mol L^{-1} for **Int0**, 7.2×10^{-6} and -2.4×10^{-6} mol L^{-1} for **Int1**^{S}, and 8.3×10^{-8} and 1.0×10^{-8} mol L^{-1} for **Int2**$_N^S$, according to the fitted

Scheme 3. Methane Amidation Experiments[a]

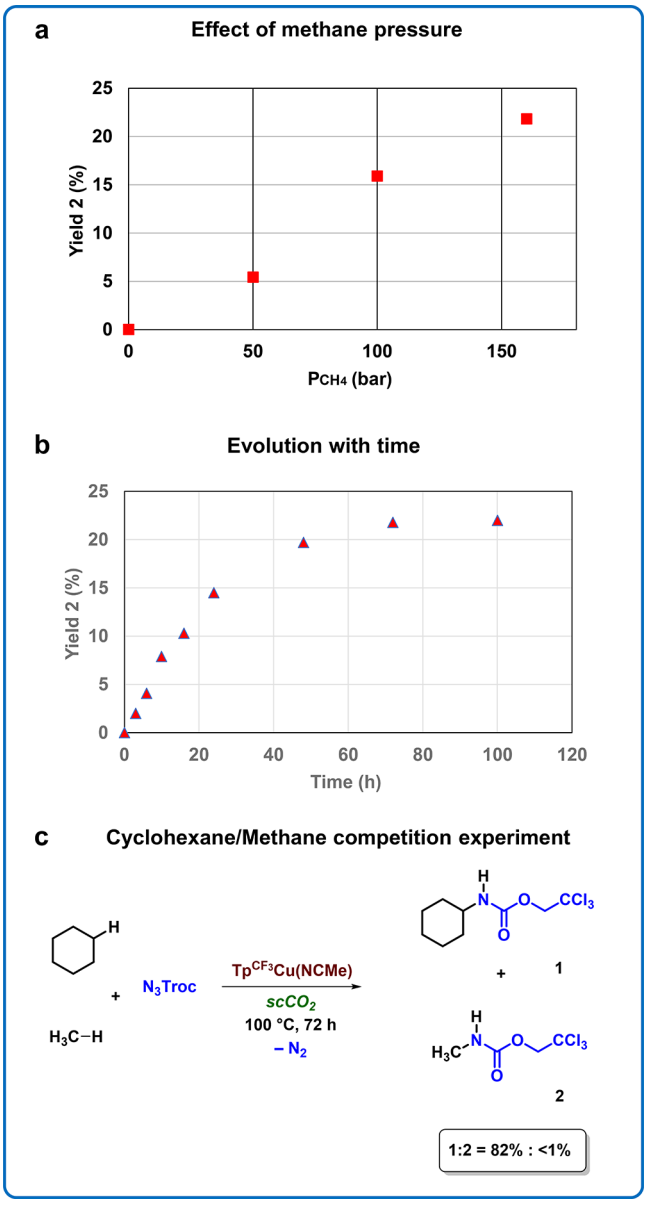

[a](a) Effect of methane pressure. (b) Monitoring of methane amidation with time. (c) Cyclohexane-methane competition experiment.

microkinetic model (373.15 K) (see Figure S18 and details in the SI). Nitrogen extrusion from **Int2**$_N^S$ occurs through **TS2−3**$_N^S$ located at 17.6 kcal mol^{-1} above **Int1**^{S} and results in the formation of molecular nitrogen and the copper nitrene intermediate **Int3**$_N^S$ in the singlet surface. The overall Gibbs free energy barrier for the formation of the copper nitrene intermediate **Int3**$_N^T$ is 29.2 kcal mol^{-1} (from **Int0**^{S} to **TS2**$_N^S$). The microkinetic model shows that this barrier is accessible under the experimental conditions and that a 2 kcal mol^{-1} larger barrier would slightly better fit the experimental results (see SI). Consequently, when experimental concentrations are considered, the process is expected to be feasible at 80 °C, with the formation of the nitrene being thermodynamically favored and kinetically viable. The nitrene intermediate is more stable as a triplet, **Int3**$_N^T$, and the crossing from the singlet to triplet surface can be done through the minimum energy crossing point

https://doi.org/10.1021/jacs.5c22747
J. Am. Chem. Soc. 2026, 148, 9057−9065

Scheme 4. Reaction Free Energy Profile for Copper Nitrene Formation and Methane Amidation[a]

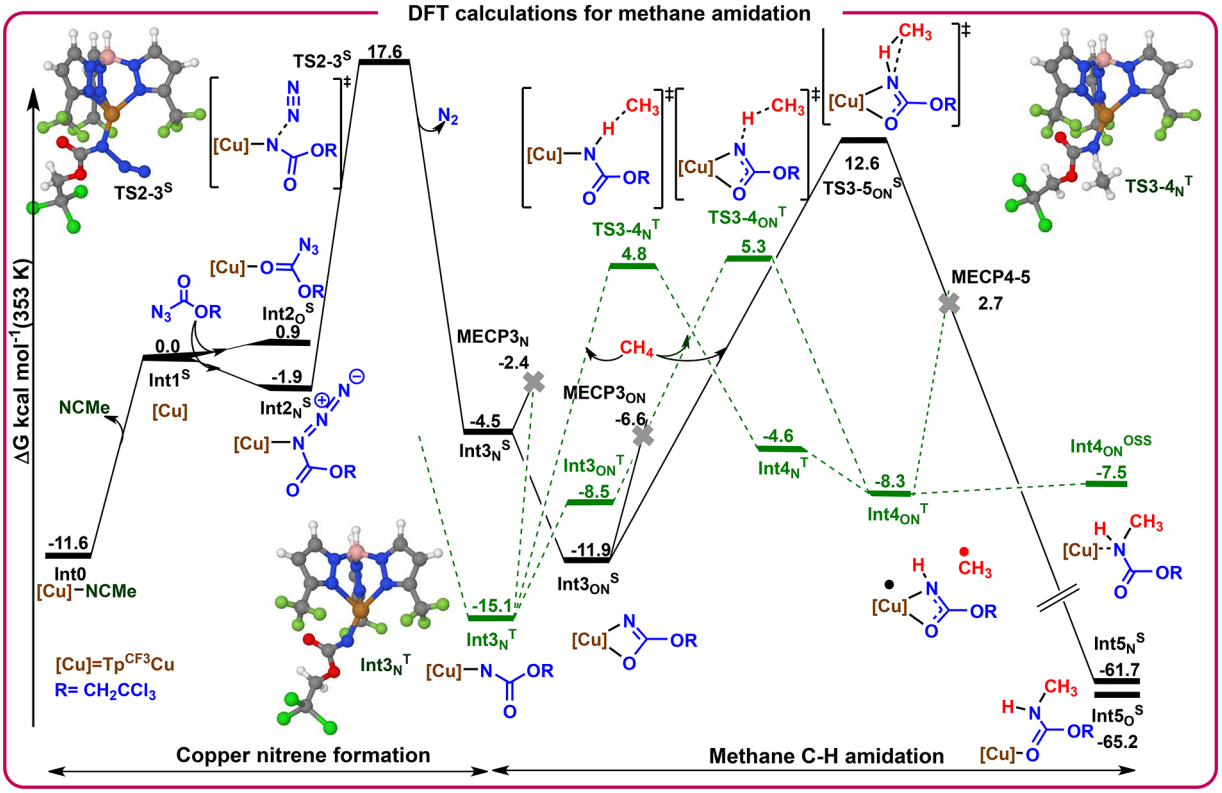

[a]Black solid lines represent the singlet surface, and green dashed lines represent the triplet surface.

Scheme 5. Schematic Comparison of the Key Transition States for Propane and i-Butane, Showing the Relative Barriers and Geometries for the Terminal and Internal C–H Bonds

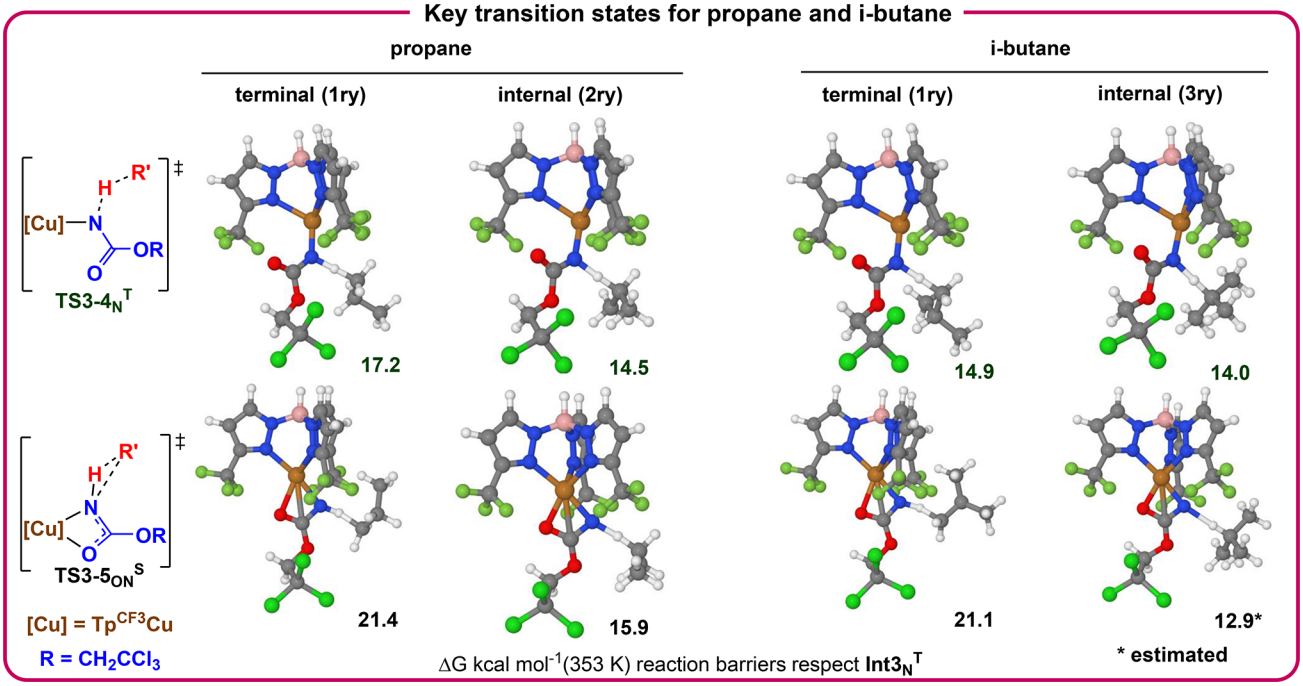

(MECP), **MECP3$_N$**. **Int3$_N$^{T}** and **MECP3$_N$** are located at −15.1 and −2.4 kcal mol^{-1} relative to **Int1^S**, respectively. The most stable copper nitrene **Int3$_N$^{T}** can isomerize upon oxygen coordination into **Int3$_{ON}$^{T}** and **Int3$_{ON}$^{S}** (which are 6.6 and 3.2 kcal mol^{-1} less stable, respectively).

The mechanism for the reaction of methane with the triplet copper nitrene **Int3$_N$^{T}** has been explored in both the triplet and singlet surfaces (Scheme 4). Transition states **TS3−4$_N$^{T}** and **TS3−4$_{ON}$^{T}**, located at 19.9 and 20.4 kcal mol^{-1} above **Int3$_N$^{T}**, activate and cleave the methane C−H bond in a homolytic

https://doi.org/10.1021/jacs.5c22747
J. Am. Chem. Soc. 2026, 148, 9057−9065

manner, generating the new N−H bond. The resulting intermediates, $\mathbf{Int4_N}^{T}$ and $\mathbf{Int4_{ON}}^{T}$, contain CH_3 and $Tp^{CF3}Cu-N(H)COOCH_2CCl_3$ radicals. The reaction further evolves with the formation of the N−CH_3 bond through **MECP4−5**, or via radical separation and rebound through the equivalent open shell singlet ($\mathbf{Int4_{ON}}^{OSS}$) to form the singlet product. **MECP4−5** is located 11.0 kcal mol^{-1} above $\mathbf{Int4_{ON}}^{T}$, 2 kcal mol^{-1} below $\mathbf{TS3-4_N}^{T}$, and leads to $\mathbf{Int5_N}^{S}$. The final product coordinates weakly to copper through oxygen, $\mathbf{Int5_O}^{S}$. Overall, the barrier associated with the formal insertion of the triplet copper nitrene to the C−H bond of methane is computationally estimated as 19.9 kcal mol^{-1} ($\mathbf{Int3_N}^{T}$ to $\mathbf{TS3-4_N}^{T}$), whereas the reaction is thermodynamically favored by 61.4 kcal mol^{-1}. We use the term formal insertion based on the composition of the final product, although the mechanism does not proceed following an insertion pathway such as that proposed for the C−H bond functionalization by carbene insertion.[26]

The singlet potential energy surface has also been evaluated, revealing a mechanistically simpler but more energy-demanding pathway. Transition state $\mathbf{TS3-5_{ON}}^{S}$ forms the N−H and N−C bonds in an asymmetric concerted way, connecting singlet copper nitrene intermediate $\mathbf{Int3_{ON}}^{S}$ with product $\mathbf{Int5_N}^{S}$. $\mathbf{TS3-5_{ON}}^{S}$ is 7.8 kcal mol^{-1} higher in energy than $\mathbf{TS3-4_N}^{T}$, and hence, amidation is expected to take place via the triplet surface.

The mechanism for ethane, propane, and *iso*-butane functionalization has also been computationally studied (Scheme 5 and Figures S4−S9), revealing that the reaction proceeds via the same pathways found for methane. In the two latter cases, the terminal and internal C−H bonds compete and lead to different products **4−5** and **8−9**, respectively. Insertion of the nitrene into the tertiary C−H bond is more favored than secondary CH_2, and both are more favored than the insertion into the primary CH_3 bonds, in good qualitative agreement with the already mentioned experimental reactivity trend. The reaction barriers from $\mathbf{Int3_N}^{T}$ to the corresponding lowest-energy triplet transition states (equivalent to $\mathbf{TS3-4_N}^{T}$) are 19.9, 16.5, 17.2, and 14.9 kcal mol^{-1} for the primary C−H bonds of methane, ethane, propane, and *i*-butane, respectively, 14.5 kcal mol^{-1} for the internal C−H bond of propane (secondary), and 14.0 kcal mol^{-1} for the internal C−H of *iso*-butane (tertiary, see SI). For ethane and propane, the preferred reaction pathway is, similar to methane, the homolytic C−H cleavage and formation of the N−H bond on the triplet surface, followed by formation of the N−C bond when crossing to the singlet surface. The largest barrier (once the nitrene is formed) is the homolytic cleavage of the C−H bond (see Scheme 5, Figures S4−S7). For *iso*-butane, the same mechanism operates for both primary and tertiary C−H bonds, but, in this case, the singlet mechanism is competitive for tertiary C−H bonds (Scheme 5). The singlet transition state for the internal C−H bond of *iso*-butane is stabilized and more asynchronous than for methane (estimated, see SI for details), presumably due to the larger stability of the corresponding carbocation.

The microkinetic models for ethane and methane as substrates are presented in detail in the SI. They are built using the above postulated computational mechanism for alkane amidation, converting computational energies to rate constants, testing different mechanistic proposals, and fitting the microkinetic model to the experimental yield for ethane and the kinetic curve of methane amidation (see Scheme 6). These models accurately reproduce the experimental data (Scheme 3b, Figure 1) and provide insight into the NTroc decomposition

Scheme 6. Construction of the Microkinetic Model for Alkane Amidation and Fitted NTroc Decomposition Side Reaction

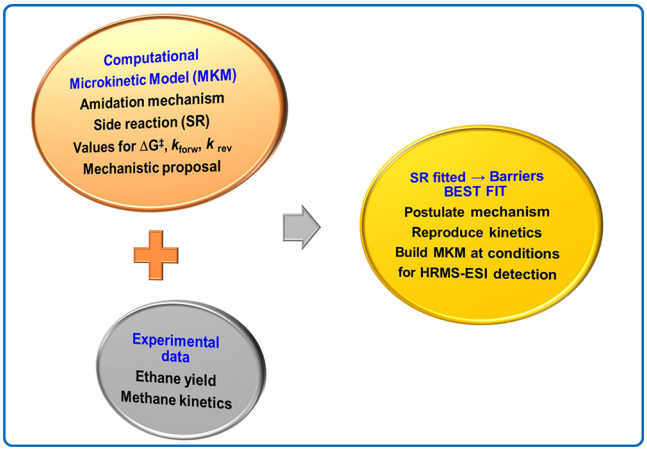

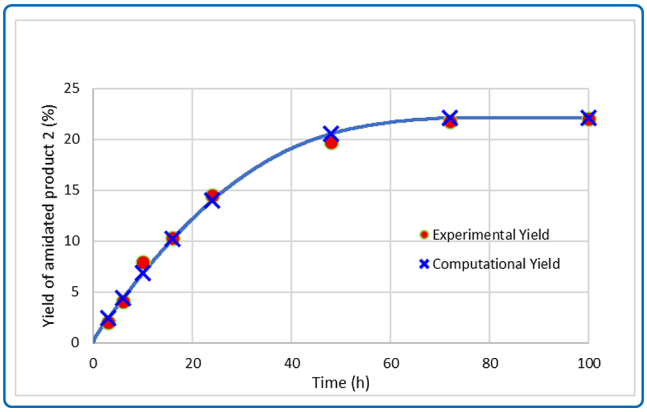

Figure 1. Fitted kinetic curve for methane amidation from the microkinetic model.

side reaction (SR). A good fit with experimental results is achieved when the side reaction mechanism consists of (i) a first selectivity-determining step that could involve water and have a barrier of 6−7 kcal mol^{-1} and (ii) a second energy-demanding step for catalyst recovery (around 30 kcal/mol).

HRMS-ESI Studies

To obtain experimental evidence supporting the calculations, we investigated the reaction of the catalyst $Tp^{CF3}Cu(NCMe)$ with N_3Troc using HRMS-ESI techniques, aiming at detecting short-lived intermediates. Thus, when a mixture of both compounds (with 0.1% MeOH added to ensure proper ionization of the sample) at room temperature was analyzed by HRMS-ESI (positive mode), two species with masses corresponding to two of the intermediates proposed from DFT calculations were detected (Scheme 7a). One of them matches that of the azide adduct $[Tp^{CF3}Cu(N_3Troc)]^+$ (**A** in Scheme 7b), whereas the other fits the mass expected for the metallonitrene $[Tp^{CF3}Cu(NTroc)]$ (**B** in Scheme 7b and $\mathbf{Int3_N}^{T}$ in calculations). It is noteworthy that when this HRMS-ESI experiment was carried out in a protic medium (MeOH), the species $[Tp^{CF3}Cu-N(H)Troc]$, resulting from the abstraction of a hydrogen atom from the medium, was detected as the result of the interception of the copper-nitrene, demonstrating the capabilities of such species to induce a HAT step in the C−H bond activation process. Calculations considering the experimental solvent and

https://doi.org/10.1021/jacs.5c22747
J. Am. Chem. Soc. 2026, 148, 9057−9065

Scheme 7. (a) Experiments for the Identification of Intermediates by HRMS-ESI; (b) Simplified Mechanism for Cyclohexane/Methanol Amidation Reactions

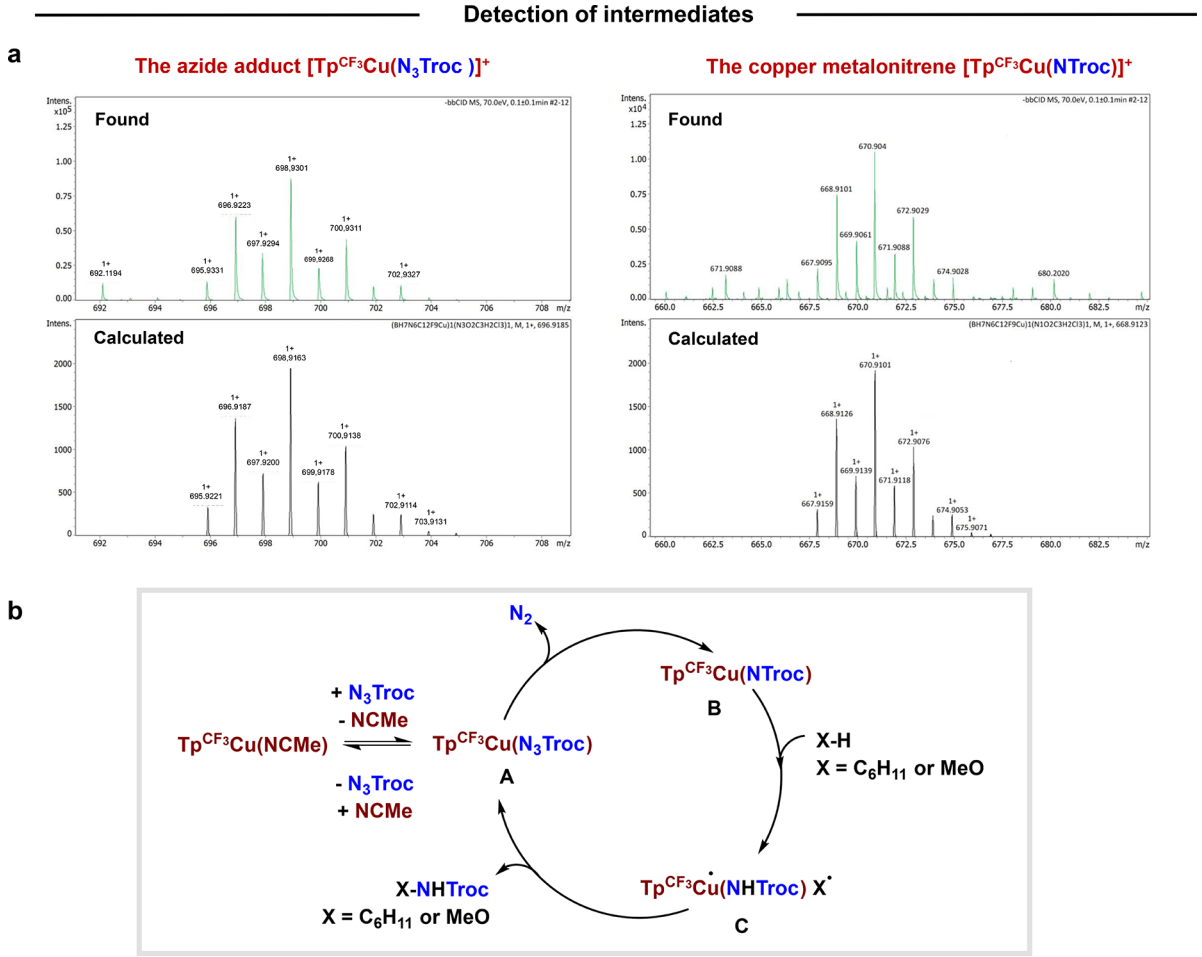

Scheme 8. (a) Competition of Cyclohexane H_{12} and D_{12} to Calculate the KIE; (b) Experiments Assessing the Intermediacy of Radical Species: Inhibition by BHT (2,6-di-t-butyl-4-hydroxytoluene) and Cyclohexyl Radical Trapping with CCl_4

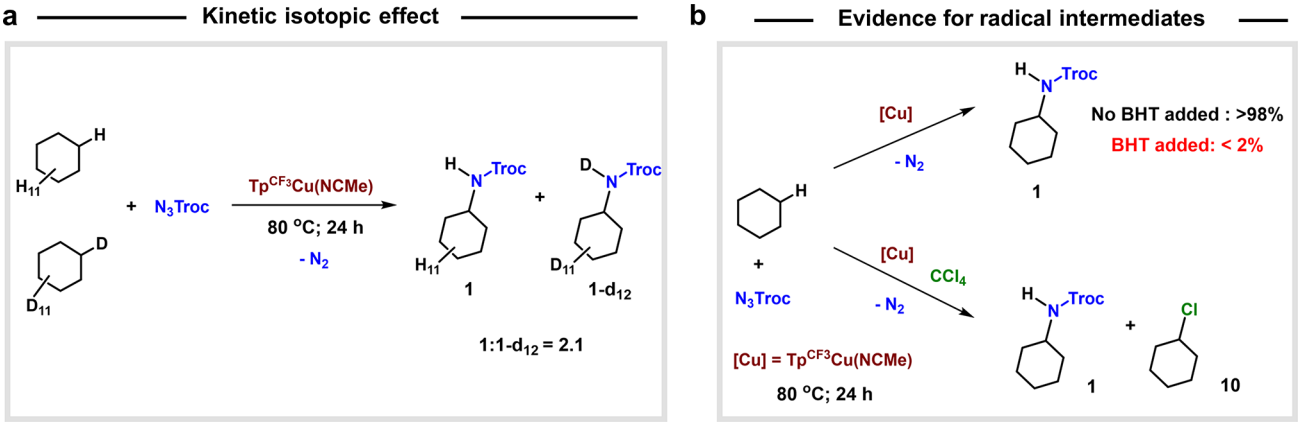

conditions for detection were performed (Figure S20) and used to build a new microkinetic model. The results show that after 10 min of reaction, the concentration of the intermediate would be of the order of 1×10^{-9} or 1×10^{-10} mol L^{-1}, depending on the model used (see Figures S21−S24 and accompanying text), and the concentration of $\mathbf{Int2_N}^S$ would be 1×10^{-9} mol L^{-1} for both models and hence detectable in HRMS-ESI.

KIE and Radical-Trap Studies

In the search for additional evidence to support the mechanistic picture, a competition experiment with cyclohexane and cyclohexane d-12 was carried out, leading to a value of KIE = 2.1 (Scheme 8a). This value is similar to that reported by Chang with a cobalt-based catalyst (2.2) and could be interpreted as the result of the homolytic C−H bond cleavage not being the rate-determining step. However, it is worth mentioning that the KIE

https://doi.org/10.1021/jacs.5c22747
J. Am. Chem. Soc. 2026, 148, 9057−9065

values reported in the literature for amidation reactions via nitrene transfer are very sensible to the electronic nature of the N-substituent: the more electron-withdrawing the substituent, the lower the KIE.[27] Therefore, comparison with other NR moieties may induce misinterpretation. The computational KIE has been estimated for secondary carbons of propane (similar to those of cyclohexane). A KIE of 4.5 was found in good qualitative agreement with experiments, which supports the postulated mechanism. Two supplementary experiments oriented to support the involvement of radical species complete this section (Scheme 8b). On one hand, the presence of a radical trap such as BHT (2,6-di-t-butyl-4-hydroxytoluene) completely inhibits the reaction. On the other hand, when CCl_4 is added instead of BHT, the cyclohexyl radical is trapped in the form of $C_6H_{11}Cl$,[28] assessing the homolytic cleavage of the cycloalkane C−H bond.

CONCLUSIONS

We have demonstrated access to catalytic methane amidation via nitrene transfer. The combination of tailored Tp^xCu-based catalysts, azide as a nitrene source, and supercritical CO_2 as the reaction medium enabled the direct, nondehydrogenative functionalization of methane upon the formal insertion of a nitrene unit into the C−H bond, a strategy that can also be applied to the other gaseous alkanes. The detection of the key copper-nitrene intermediate provides experimental evidence of the DFT-calculated mechanism. In view of the similarities between oxo- and nitrene-transfer reactions from copper centers,[29,30] we believe that these results constitute an excellent foundation for the related and more challenging direct oxidation of methane into methanol via oxo insertion into the C−H bond of methane and will inspire further research in this direction.

ASSOCIATED CONTENT

Supporting Information

The Supporting Information is available free of charge at https://pubs.acs.org/doi/10.1021/jacs.5c22747.

All procedures and characterization data for new compounds, catalytic experiments, and DFT calculations (PDF)

AUTHOR INFORMATION

Corresponding Authors

Maria Besora − *Departament de Química Física i Inorgànica, Universitat Rovira i Virgili, 43007 Tarragona, Spain;* orcid.org/0000-0002-6656-5827; Email: maria.besora@urv.cat

María Álvarez − *Laboratorio de Catálisis Homogénea, Unidad Asociada al CSIC, CIQSO-Centro de Investigación en Química Sostenible and Departamento de Química, Universidad de Huelva, 21007 Huelva, Spain*; Email: maria.alvarez@dqcm.uhu.es

Ana Caballero − *Laboratorio de Catálisis Homogénea, Unidad Asociada al CSIC, CIQSO-Centro de Investigación en Química Sostenible and Departamento de Química, Universidad de Huelva, 21007 Huelva, Spain;* orcid.org/0000-0001-7846-6183; Email: ana.caballero@dqcm.uhu.es

Pedro J. Pérez − *Laboratorio de Catálisis Homogénea, Unidad Asociada al CSIC, CIQSO-Centro de Investigación en Química Sostenible and Departamento de Química, Universidad de Huelva, 21007 Huelva, Spain;* orcid.org/0000-0002-6899-4641; Email: perez@dqcm.uhu.es

Authors

Jonathan Martínez-Laguna − *Laboratorio de Catálisis Homogénea, Unidad Asociada al CSIC, CIQSO-Centro de Investigación en Química Sostenible and Departamento de Química, Universidad de Huelva, 21007 Huelva, Spain*

Anna Cholewinska − *Departament de Química Física i Inorgànica, Universitat Rovira i Virgili, 43007 Tarragona, Spain*

Elena Borrego − *Laboratorio de Catálisis Homogénea, Unidad Asociada al CSIC, CIQSO-Centro de Investigación en Química Sostenible and Departamento de Química, Universidad de Huelva, 21007 Huelva, Spain*

Complete contact information is available at: https://pubs.acs.org/10.1021/jacs.5c22747

Notes

The authors declare no competing financial interest.

ACKNOWLEDGMENTS

We thank the Spanish Ministerio de Ciencia e Innovación for grants TED 2021-130077B-100 (PJP), PID2020-113797RB-C21 (PJP, AC), PID2023-146946NB-I00 (PJP), RED2022-134074-T (PJP), CN2022-136079 (MB), PID2021-128188NB-100 (MB), and the Catalan Agency for Research (AGAUR) 021 SGR 00110 (MB). We also thank Universidad de Huelva/CBUA for open access charges.

REFERENCES

(1) Gunsalus, N. J.; Koppaka, A.; Park, S. H.; Bishof, S. M.; Hashigushi, B. G.; Periana, R. A. Homogeneous Functionalization of Methane. *Chem. Rev.* **2017**, *117*, 8521−8573.

(2) Caballero, A.; Pérez, P. J. Methane as raw material in synthetic chemistry: the final frontier. *Chem. Soc. Rev.* **2013**, *42*, 8809−8820.

(3) Luo, Y.-R. *Comprehensive Handbook of Chemical Bond Energies*; CRC Press: Boca Ratón, 2007.

(4) Pauling, L. The nature of the chemical bond. IV. The energy of single bonds and the relative electronegativity of atoms. *J. Am. Chem. Soc.* **1932**, *54*, 3570−3582.

(5) Periana, R. A.; Taube, D. J.; Evitt, E. R.; Loffler, D. G.; Wentrcek, P. R.; Voss, G.; Masuda, T. A mercury-catalyzed, high-yield system for the oxidation of methane to methanol. *Science* **1993**, *259*, 340−343.

(6) Periana, R. A.; Taube, D. J.; Gamble, S.; Taube, H.; Satoh, T.; Fujii, H. Platinum catalysts for the high-yield oxidation of methane to a methanol derivative. *Science* **1998**, *280*, 560−564.

(7) Smith, K. T.; Berritt, S.; González-Moreiras, M.; Ahn, S.; Smith, M. R., III; Baik, M.-H.; Mindiola, D. J. Catalytic borylation of methane. *Science* **2016**, *351*, 1424−1427.

(8) Cook, A. K.; Schimler, S. D.; Matzger, A. J.; Sanford, M. S. Catalyst-controlled selectivity in the C-H borylation of methane and ethane. *Science* **2016**, *351*, 1421−1424.

(9) Sadow, A. D.; Tilley, T. D. Catalytic Functionalization of Hydrocarbons by σ-Bond-Metathesis Chemistry: Dehydrosilylation of Methane with a Scandium Catalyst. *Angew. Chem., Int. Ed.* **2003**, *42*, 803−805.

(10) Sadow, A. D.; Tilley, T. D. Homogeneous Catalysis with Methane. A Strategy for the Hydro-methylation of Olefins Based on the Nondegenerate Exchange of Alkyl Groups and σ-Bond Metathesis at Scandium. *J. Am. Chem. Soc.* **2003**, *125*, 7971−7977.

(11) Fujisaki, H.; Ishizuka, T.; Kotani, H.; Shiota, Y.; Yoshizawa, K.; Kojima, T. Selective methane oxidation by molecular iron catalysts in aqueous medium. *Nature* **2023**, *616*, 476−481.

(12) Cosio, M. N.; Powers, D. C. Prospects and challenges for nitrogen-atom transfer catalysis. *Nat. Rev. Chem.* **2023**, *7*, 424−438.
(13) Michos, D.; Sassano, C. A.; Krajnik, P.; Crabtree, R. H. Amination of Methane and Ethane by Mercury Photosensitization in the Presence of Ammonia. *Angew. Chem., Int. Ed. Engl.* **1993**, *32*, 1491−1492.
(14) Hu, A.; Guo, J.-J.; Zuo, Z. Selective functionalization of methane, ethane, and higher alkanes by cerium photocatalysis. *Science* **2018**, *361*, 668−672.
(15) Fuentes, M. A.; Gava, R.; Saper, N. I.; Romero, E. A.; Caballero, A.; Hartwig, J. F.; Pérez, P. J. Copper-Catalyzed Dehydrogenative Amidation of Light Alkanes. *Angew. Chem., Int. Ed.* **2021**, *60*, 18467−18471.
(16) Gunsalus, N. J.; Park, S. H.; Hashigushi, B. G.; Koppaka, A.; Smith, S. J.; Ess, D. H.; Periana, R. H. Selective N Functionalization of Methane and Ethane to Aminated Derivatives by Main-Group-Directed C−H Activation. *Organometallics* **2019**, *38*, 2319−2322.
(17) Badiel, Y. M.; Dinescu, A.; Dai, X.; Palomino, R. M.; Heinemann, F. W.; Cundari, T. R.; Warren, T. H. Copper−Nitrene Complexes in Catalytic C-H Amination. *Angew. Chem., Int. Ed.* **2008**, *47*, 9961−9964.
(18) Gómez-Emeterio, B. P.; Urbano, J.; Díaz-Requejo, M. M.; Pérez, P. J. Easy Alkane Catalytic Functionalization. *Organometallics* **2008**, *27*, 4126−4130.
(19) Liang, C.; Collet, F.; Robert-Peillard, F.; Müller, P.; Dodd, R. H.; Dauban, P. Toward a Synthetically Useful Stereoselective C−H Amination of Hydrocarbons. *J. Am. Chem. Soc.* **2008**, *130*, 343−350.
(20) Lee, J.; Jin, S.; Kim, D.; Hong, S. H.; Chang, S. Cobalt-Catalyzed Intermolecular C−H Amidation of Unactivated Alkanes. *J. Am. Chem. Soc.* **2021**, *143*, 5191−5200.
(21) Fructos, M. R.; Trofimenko, S.; Díaz-Requejo, M. M.; Pérez, P. J. Facile Amine Formation by Intermolecular Catalytic Amidation of Carbon−Hydrogen Bonds. *J. Am. Chem. Soc.* **2006**, *128*, 11784−11791.
(22) Rodríguez, A. M.; Pérez-Ruíz, J.; Molina, F.; Poveda, A.; Pérez-Soto, R.; Maseras, F.; Díaz-Requejo, M. M.; Pérez, P. J. Introducing the Catalytic Amination of Silanes via Nitrene Insertion. *J. Am. Chem. Soc.* **2022**, *144*, 10608−10614.
(23) Caballero, A.; Despagnet-Ayoub, E.; Díaz-Requejo, M. M.; Díaz-Rodríguez, A.; González-Núñez, M. E.; Mello, R.; Muñoz, B. K.; Ojo, W. S.; Asensio, G.; Etienne, M.; Pérez, P. J. Silver-catalyzed C-C bond formation between methane and ethyl diazoacetate in supercritical CO_2. *Science* **2011**, *332*, 835−838.
(24) Olmos, A.; Asensio, G.; Pérez, P. J. Homogeneous Metal-Based Catalysis in Supercritical Carbon Dioxide. *ACS Catal.* **2016**, *6*, 4265−4280.
(25) Alvarez-Moreno, M.; de Graaf, C.; Lopez, N.; Maseras, F.; Poblet, J. M.; Bo, C. Managing the Computational Chemistry Big Data Problem: The ioChem-BD Platform. *J. Chem. Inf. Model.* **2015**, *55*, 95−103.
(26) Olmos, A.; Gava, R.; Noverges, B.; Bellezza, D.; Jacob, K.; Besora, M.; Sameera, W. M. C.; Etienne, M.; Maseras, F.; Asensio, G.; Caballero, A.; Pérez, P. J. Measuring the Relative Reactivity of the Carbon-Hydrogen Bonds of Alkanes as Nucleophiles. *Angew. Chem., Int. Ed.* **2018**, *57*, 13848−13852.
(27) Bagchi, V.; Paraskevopoulou, P.; Das, P.; Chi, L.; Wang, Q.; Choudhury, A.; Mathieson, J. S.; Cronin, L.; Pardue, D. B.; Cundari, T. R.; Mitrikas, G.; Sanakis, Y.; Stavropoulos, P. A Versatile Tripodal Cu(I) Reagent for C-N Bond Construction Via Nitrene-Transfer Chemistry: Catalytic Perspectives and Mechanistic Insights on C-H Aminations/Amidinations and Olefin Aziridinations. *J. Am. Chem. Soc.* **2014**, *136*, 11362−11381.
(28) Mahy, J. P.; Bedi, G.; Battioni, P.; Mansuy, D. Amination of alkanes catalyzed by iron-porphyrins and manganese-porphyrins - particular selectivity for omega-1 and omega-1 oxidations of linear alkanes. *New J. Chem.* **1989**, *13*, 651−657.
(29) Conde, A.; Vilella, L.; Balcells, D.; Díaz-Requejo, M. M.; Lledós, A.; Pérez, P. J. Introducing Copper as Catalyst for Oxidative Alkane Dehydrogenation. *J. Am. Chem. Soc.* **2013**, *135*, 3887−3896.
(30) Hou, K.; Hrovat, D. A.; Bao, X. Computational exploration of the mechanism of copper-catalyzed aromatic C−H bond amination of benzene via a nitrene insertion approach. *Chem. Commun.* **2015**, *51*, 15414−15417.

https://doi.org/10.1021/jacs.5c22747
J. Am. Chem. Soc. 2026, 148, 9057−9065